Muscles from the same muscle group do not necessarily share common drive: evidence from the human triceps surae

François Hug, Alessandro del Vecchio, Simon Avrillon, Dario Farina, Kylie Tucker

J Appl Physiol 130: 342–354, 2021.
First published November 26, 2020; doi:10.1152/japplphysiol.00635.2020

american physiological society

JOURNAL OF APPLIED PHYSIOLOGY

RESEARCH ARTICLE

Muscles from the same muscle group do not necessarily share common drive: evidence from the human triceps surae

François Hug,[1,2,3] Alessandro Del Vecchio,[4,5] Simon Avrillon,[2,6,7] Dario Farina,[4] and Kylie Tucker[2]

[1]*Laboratory "Movement, Interactions, Performance" (EA 4334), Nantes University, Nantes, France;* [2]*School of Biomedical Sciences, The University of Queensland, Brisbane, Australia;* [3]*Institut Universitaire de France (IUF), Paris, France;* [4]*Neuromechanics and Rehabilitation Technology Group, Department of Bioengineering, Faculty of Engineering, Imperial College London, London, United Kingdom;* [5]*Department of Artificial Intelligence in Biomedical Engineering, Friedrich-Alexander University, Erlangen-Nürnberg, Erlangen,Germany;* [6]*Legs + Walking AbilityLab, Shirley Ryan AbilityLab, Chicago, Illinois; and* [7]*Department of Physical Medicine and Rehabilitation, Northwestern University, Chicago, Illinois*

Abstract

It has been proposed that movements are produced through groups of muscles, or motor modules, activated by common neural commands. However, the neural origin of motor modules is still debated. Here, we used complementary approaches to determine: *1*) whether three muscles of the same muscle group [soleus, gastrocnemius medialis (GM), and gastrocnemius lateralis (GL)] are activated by a common neural drive, and *2*) whether the neural drive to GM and GL could be differentially modified by altering the mechanical requirements of the task. Eighteen human participants performed an isometric standing heel raise and submaximal isometric plantarflexions (10%, 30%, and 50% of maximal effort). High-density surface electromyography recordings were decomposed into motor unit action potentials and coherence analysis was applied on the motor unit spike trains. We identified strong common drive to each muscle but minimal common drive between the muscles. Further, large between-muscle differences were observed during the isometric plantarflexions, such as a delayed recruitment time of GL compared with GM and soleus motor units and opposite time-dependent changes in the estimates of neural drive to muscles during the torque plateau. Finally, the feet position adopted during the heel-raise task (neutral vs. internally rotated) affected only the GL neural drive with no change for GM. These results provide conclusive evidence that not all anatomically defined synergist muscles are controlled by strong common neural drive. Independent drive to some muscles from the same muscle group may allow for more flexible control to comply with secondary goals such as joint stabilization.

NEW & NOTEWORTHY In this study, we demonstrated that the three muscles composing the human triceps surae share minimal common drive during isometric contractions. Our results suggest that reducing the number of effectively controlled degrees of freedom may not always be the strategy used by the central nervous system to control movements. Independent control of some, but not all, synergist muscles may allow for more flexible control to comply with secondary goals (e.g., joint stabilization).

coherence; common drive; electromyography; gastrocnemius; motor units

INTRODUCTION

How the central nervous system controls the large number of degrees of freedom of the musculoskeletal system to produce movements remains unclear. It has been proposed that muscles are controlled through motor modules, which represent groups of muscles, activated by a single neural command (1–3). Evidence for the existence of motor modules, which reduce the dimensionality in the control of movement, comes from animal models where cortical (4) or spinal microstimulation (5) led to complex multijoint forces. However, the neural origin of motor modules is still debated (6, 7).

In support of the modular control of movements, there is evidence that some muscles are controlled primarily by a shared neural drive (8–11) and that the intensity of this shared drive is stronger between muscles that are anatomically and functionally closely related (9, 10). Considering the behavior of a population of motor units identified from high-density surface electromyography (HDsEMG), Laine et al. (11) demonstrated that the lateral (vastus lateralis [VL]) and medial (vastus medialis [VM]) head of the quadriceps share most of their synaptic input during isometric knee extension. Given the important role of VL and VM in the control of the patellofemoral joint (12), this shared common input might achieve two important goals: *1*) simplify the control of the task and *2*) regulate internal joint stresses. Although a shared drive may be an optimal control strategy for the VL and VM muscles, it might not be optimal for muscles that require more flexible control.

The *triceps surae* consists of the soleus (SOL), gastrocnemius medialis (GM), and gastrocnemius lateralis (GL). As GM and GL

Correspondence: F. Hug (francois.hug@univ-nantes.fr).
Submitted 23 July 2020 / Revised 4 November 2020 / Accepted 11 November 2020

share the same two main functions (plantarflexion and knee flexion), and both insert into the Achilles tendon, they are very often regarded as the same muscle (13). In addition, using factorization of multiple bipolar EMG signals, these muscles are consistently reported as part of the same module [e.g., gait (14), pedaling (15)]. However, there is some indirect evidence that GM and GL may produce different ankle torques in the frontal plane (16, 17). As such, flexibility in their control with minimal common drive, i.e., the ability to activate the muscles independently, might be crucial for maintaining balance or producing force in different directions. For example, Héroux et al. (18) observed a difference in GM and GL motor unit discharge behavior during standing balance, with a relative absence of GL motor unit activity. Taken together, these results suggest that the activation of the GM and GL muscles may be partly independent, with a small amount of common drive, to allow for flexible control of the ankle joint.

In this study, we used multiple and complementary approaches to characterize the behavior of populations of motor neurons innervating the three heads of the *triceps surae*, with specific consideration of GM and GL. Our primary aim was to determine whether GL and GM share a common neural drive during plantarflexion. We first estimated the within- and between-muscle common neural drive using correlation techniques in the frequency domain [i.e., coherence (19, 20] applied to motor unit spike trains identified from an isometric heel-raise task. Then, we assessed motor unit discharge characteristics during isometric plantarflexions performed on an ergometer. Our secondary aim was to determine whether the neural drive to GM and GL could be differentially modified by altering the mechanical requirements of the task. For this purpose, we compared the motor unit discharge rate between two heel-raise tasks performed with different feet positions. We hypothesized that the GM and GL muscles share minimal common drive and, therefore, that the neural drive to the GM and GL can be independently altered. If supported, this would provide strong evidence that some anatomically derived synergist muscles can be controlled by independent neural drive and would force a reconsideration of our understanding of the modular control of movement.

METHODS

Participants

Eighteen physically active males participated in this study (means ± SD; age, 29.4 ± 7.9 yr; height, 180 ± 7 cm; body mass, 76 ± 8 kg; body mass index, 23.6 ± 2.7 kg/m^2). Of note, we were not avoiding recruiting females; but for unknown reasons, we failed to identify enough motor units on females during our pilot testing, especially on GL. Participants had no history of lower leg pain that had limited function that required time off work or sport or a consultation with a health practitioner in the previous 6 months. The institutional research ethics committee of the University of Queensland approved this study (n°2013001448), and all procedures adhered to the Declaration of Helsinki. Participants provided informed written consent.

Experimental Design

The experimental session consisted of a series of isometric and postural tasks. The myoelectrical activity of the three heads of the *triceps surae* of the dominant leg (right/left; 16/2) was measured using HDsEMG.

First, participants laid prone on a custom-made dynamometer equipped with a torque sensor (TRE-50K, Dacell, Korea; Fig. 1). Their knee was fully extended, and their ankle angle was set to 10° of plantarflexion (0° being the foot perpendicular to the shank). The experiment began with a warm-up, which included a series of submaximal contractions. Then, participants performed three maximal isometric contractions for 3–5 s with 120-s rest in between. The maximal value obtained from a moving average window of 250 ms was considered as the peak torque (MVC). Then, participants performed three contractions at each of the following intensities: 10%, 30%, and 50% of their MVC. The order of the intensities was randomized. These contractions involved a 5-s ramp-up, a 15-s (50% of MVC) or 20-s plateau (10% and 30% of MVC), and a 5-s ramp-down phase. The contractions were separated by either 60 s (10% of MVC) or 120 s (30% and 50% of MVC) of rest. Feedback of the target and torque output was displayed on a monitor.

Second, participants stood barefoot on a force plate (Model 4060, Bertec, UK) and performed a series of six tasks in a randomized order, including balance and heel-raise tasks. The balance tasks were performed for another purpose. For the purpose of this study, only the two isometric heel-raise tasks were analyzed. These tasks consisted of holding the heel at a standard height of 6 cm, with both feet in a neutral position (toes neutral) or internally rotated (toes in) (Fig. 1). To provide feedback of the height, a 6-cm-thick piece of high-density foam was placed under the heels of the participants. The participants were instructed to lightly touch the top of the foam with their heels and once the correct height was achieved (in typically less than 5 s), the piece of foam was removed, and data collection began. For the toes neutral condition, the participants adopted a comfortable stance width with their feet pointing anteriorly. For the toes in condition, the participants pointed their toes inward by internally rotating their lower limbs, such that their feet formed an angle of 90°. About 1/4 of the participants could not reach this angle, in which case they were instructed to rotate their lower limbs as far as possible. Each of these conditions was repeated two times for 30–35 s with 15–20 s of rest in between.

For both the plantarflexion tasks performed on the ergometer and the heel-raise tasks, the mechanical signals (torque and force) were digitized at 2048 Hz using the same acquisition system as that used for HDsEMG (EMG-Quattrocento; 400-channel EMG amplifier, OT Biolelettronica, Italy).

Note that additional measurements were performed on the VL and VM muscles for two participants (*participant 5* and *participant 10*). These participants performed an isometric body-weight squat (knee angle = 30°; 0 = knee fully extended) for 3 × 30 s.

High-Density Surface EMG Recordings

HDsEMG signals were recorded from the GL, GM, and SOL muscles. Two-dimensional adhesive grids of 64 electrodes (13 × 5 electrodes with one electrode absent on a corner, gold-coated, interelectrode distance, 8 mm; [ELSCH064NM2, SpesMedica, Battipaglia, Italy]) were placed over both the GM

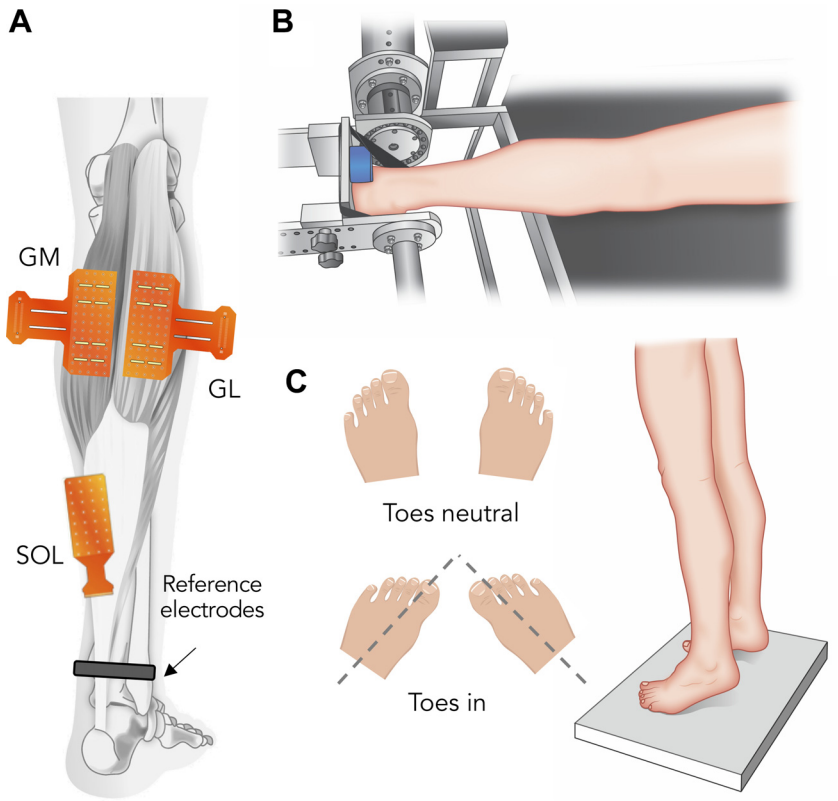

Figure 1. Experimental setup. *A*: shows the placement of the high-density electromyography electrodes. A two-dimensional adhesive grid of 64 electrodes was placed over both the gastrocnemius medialis (GM) and the gastrocnemius lateralis (GL) muscle. A two-dimensional adhesive grid of 32 electrodes was placed on the medial part of the soleus (SOL), below the myotendinous junction of the GM muscle. *B*: shows the isometric plantarflexion task performed on the ergometer (knee was fully extended and ankle angle at 10° of plantarflexion). *C*: shows the isometric heel-raise task which consisted of holding the heel at a standard height of 6 cm, with either the feet in neutral position (comfortable stance; toes neutral) or internally rotated (toes in).

and the GL muscle (Fig. 1). The grids were aligned with the main fascicle direction as determined using B-mode ultrasound (Aixplorer, Supersonic Imagine, France). A two-dimensional adhesive grid of 32 electrodes (8×4 electrodes, gold-coated, interelectrode distance, 10 mm; [GR10MM0804, SpesMedica, Battipaglia, Italy]) was placed on the medial part of the SOL, below the myotendinous junction of the GM muscle (Fig. 1). This electrode was aligned with the supposed line of action of the muscle. Before electrode application, the skin was shaved, and then cleaned with an abrasive pad and alcohol. The adhesive grids were held on the skin using semi-disposable bi-adhesive foam layers (SpesMedica, Battipaglia, Italy). The skin-electrode contact was made by filling the cavities of the adhesive layers with conductive paste (SpesMedica, Battipaglia, Italy). An 8-cm-wide elastic band was placed over the three electrodes with a slight tension to ensure that all the electrodes remained in contact with the skin throughout the experiment. Strap electrodes dampened with water were placed around the contralateral (ground electrode) and ipsilateral ankle (reference electrode). The EMG signals were recorded in monopolar mode, bandpass filtered (10–900 Hz), and digitized at a sampling rate of 2048 Hz using a multichannel acquisition system (EMG-Quattrocento; 400-channel EMG amplifier, OT Biolelettronica, Italy).

Data Analysis

In this study, we considered the neural drive as the ensemble of motor neuron discharges, and this drive was estimated using the cumulative spike train (CST, sum of the motor unit discharge times) of a subset of motor neurons identified by decomposition. Common drive was considered as the component of the neural drive that is shared between motor neurons, i.e., the common (correlated) fluctuations of motor unit discharge timings.

Global EMG.

EMG signals were band-pass filtered (20–500 Hz), differentiated, and full-wave rectified. For the MVC trials, the EMG amplitude was calculated over a moving time window of 500 ms. The resulting highest value over the three contractions and over all the channels of the grid was considered as the maximal EMG amplitude value. For the submaximal tasks, the EMG amplitude was calculated over the whole contraction, averaged across all channels, and normalized to that determined during the maximal isometric contractions.

HDsEMG decomposition.

First, the monopolar EMG signals were bandpass filtered between 20 and 750 Hz with a second-order Butterworth filter. The HDsEMG signals were decomposed with the convolutive blind source separation method (21) implemented in the DEMUSE tool software (v. 4.9; The University of Maribor, Slovenia). This decomposition procedure can identify motor unit discharge times over a wide range of contraction intensities and has been extensively validated using experimental and simulated signals (22, 23). After the automatic identification of the motor units, all the motor unit spike trains were visually inspected (24, 25). As classically done, only the motor units that exhibited a pulse-to-noise ratio > 30 dB were retained for further analysis (11, 26). This threshold ensured a sensitivity higher than 90% and a false-alarm rate lower than 2% (23).

Assessment of cross talk.

Before assessing the neural connectivity between the different populations of motor neurons of the *triceps surae*, we used the discharge timings extracted by decomposition to assess the uniqueness of the motor unit action potentials. This was done to guarantee that each motor unit that was used for subsequent analysis originated from the target muscles on which the high-density EMG grid was placed and was not a result of cross talk from a neighboring muscle. For this purpose, the discharge timings of each motor unit extracted by decomposition were used to trigger all of the HDsEMG signals (64 [GM] +64 [GL] +32 [SOL] channels). The motor unit action potentials extracted by spike trigger averaging were then compared between muscles. Specifically, we calculated the average amplitude of the motor unit action potential, for each HDsEMG grid, by averaging the peak-to-peak amplitude across all channels of each HDsEMG grid. We then compared this average peak-to-peak amplitude between grids to identify motor units that originated from cross talk. This analysis assumes that the action potential representation of a motor unit will be largest when recorded from the electrodes placed on the muscle of origin. Conversely, motor units that are identified from a neighboring muscle will have a smaller peak-to-peak amplitude due to a greater distance between the electrodes and the muscle unit (25). As such, if the average peak-to-peak amplitude of a motor unit was higher in one of the muscles from where this unit was not originally identified, this unit was visually inspected and then omitted from the analysis.

Within- and between-muscle coherence.

We used a coherence analysis to assess the neural connectivity between motor units from the same (within-muscle coherence) or from different muscles (between-muscle coherence) (27). Note that coherence calculated at a given frequency represents the correlation between the two signals at that frequency, with 0 indicating noncorrelation and 1 indicating perfect correlation. Coherence within the δ band (0–5 Hz) reflects the presence of common drive (11, 25, 28).

Because the GL motor units were recruited late during the plateau of the isometric plantarflexion tasks performed on the ergometer (see RESULTS), the number of discharges was too low to conduct coherence analysis on these tasks. In other words, too few motor units were recruited during enough time to run a meaningful coherence analysis. Thus, the coherence analysis was only performed on the isometric heel-raise task, with toes neutral, as this was the condition during which the greatest number of motor units was identified for both GM and GL.

Prior to this coherence analysis, the discharge times of each motor unit were visually inspected. Even if it was not frequently observed, pauses in the recruitment of some motor units occasionally occurred. Such pauses can affect the calculation of the coherence. Therefore, if one motor unit exhibited a pause in discharges for >2 s, this portion of the signal was discarded for all motor units. If for a given unit these pauses occurred too often, that motor unit was not considered such that the analysis could still be performed on all other units. On average, the coherence analysis was performed on 54 ± 16 s and 47 ± 13 s, for within-muscle and between-muscle coherence, respectively.

For the within-muscle coherence, we calculated the magnitude-squared coherence using the Welch periodogram with nonoverlapping windows of 1 s (Fig. 2). This analysis was performed on two equal-sized groups of CST. The number of motor units in each of the two groups varied from 1 to the maximum number (half of the total number of identified units), and 100 random permutations of the identified units were performed for each iteration. Then, we estimated the proportion of common synaptic input to motor neurons using the method described by Negro et al. (29). For this analysis, we focused on the low-frequency bandwidth (0–5 Hz), as it has been shown to be the main determinant of the force output (19). The relationship between the average values of coherence in the bandwidth 0–5 Hz and the number of motor units was fitted by least-squares using a nonlinear equation described by Negro et al. (29). The rate of change (the slope) was considered as the proportion of common input (PCI) with respect to the total input received by the motor neuron pool (Fig. 2) (29). This method was validated in numerical simulations, which were based on a model of populations of motor neurons that received common and independent inputs (29). The advantage of this method is to provide a quantitative estimate of the relative strength of the common synaptic input, independent of the number of identified units, allowing us to make direct comparisons between muscles.

The between-muscle coherence was assessed in a similar way as the within-muscle coherence. Specifically, the total number of identified motor units was used to generate the CST. Then, we applied the coherence function between the CST for each muscle pair (GM-GL, GM-SOL, GL-SOL). Coherence was considered significant when it was higher than the maximum value of coherence for frequencies >100 Hz, where no coherence is expected (30). In addition, we considered the presence of substantial common neural drive if the coherence values reached this significance threshold over the entire bandwidth 0–5 Hz.

Motor unit discharge characteristics.

To compare the neural drive received by the three muscles during the isometric plantarflexions performed on the ergometer, we calculated three indexes (Fig. 3). First, the time of recruitment of each motor unit was determined for each contraction as the time when the first action potential was observed (Fig. 3). As these tasks involved a 5-s ramp-up phase before the torque plateau, a value higher than 5 s indicated that the motor unit was recruited during the plateau. As expected, most of GM and SOL motor units were recruited during the ramp-up phase, but surprisingly, most of the GL motor units were recruited during the plateau (Fig. 3). Therefore, we were unable to consider the joint torque associated with recruitment (i.e., the recruitment threshold), as classically done. Second, we determined the δ discharge rate (expressed in pps $\cdot$ S^{-1}) to provide an estimate of the synaptic inputs received by the motor neuron pools (31). This was calculated as the rate of change in discharge rate within the first 2 s of recruitment (Fig. 3). Because variability in instantaneous discharge rate may occur at recruitment, we considered

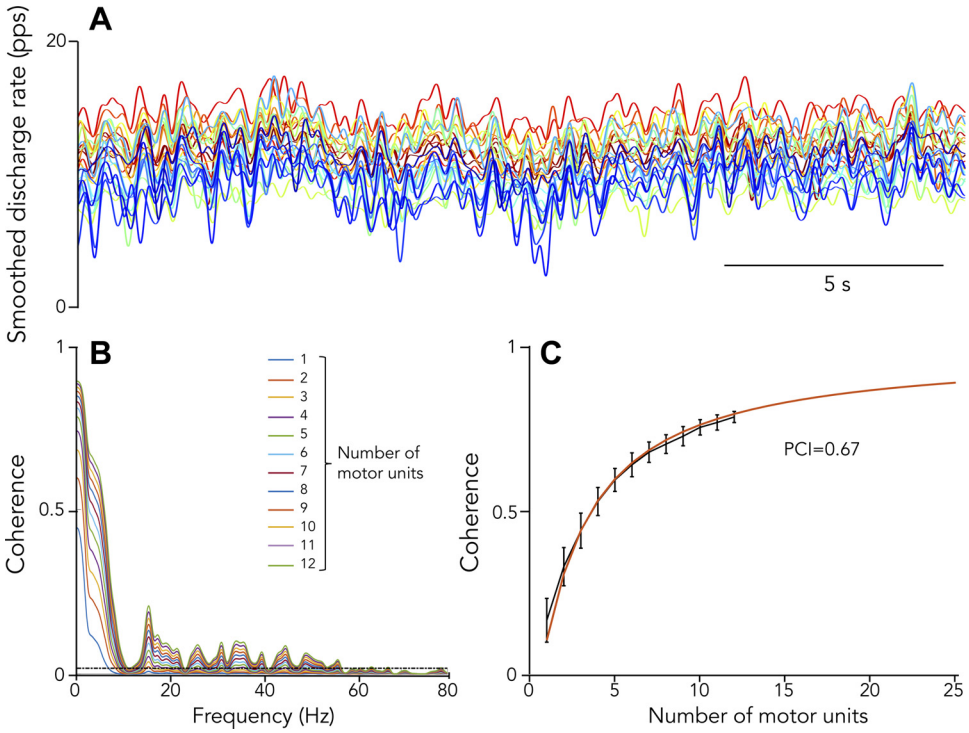

Figure 2. Individual example of the assessment of the proportion of common input (PCI). *A*: shows the smoothed discharge rate (cut-off frequency = 2 Hz) of 25 motor units identified from the gastrocnemius medialis, during the isometric heel-raise task performed with the toes in neutral position, for *participant 12*. Note that only 20 s of the contraction are depicted here. *B*: shows the results of the coherence analyses performed on two cumulative spike trains, with varying number of motor units in each group, i.e., from 1 to 12 motor units. Each estimation is the average of 100 random permutations of motor units. The horizontal line indicates the threshold of significant coherence for 12 motor units per group. *C*: represents the relationship between the mean values (±standard deviation) of coherence in the bandwidth 0–5 Hz and the number of motor units. This relationship was fitted by least-squares (red line) and the rate of change was considered as an index of the proportion of common input (PCI).

the discharge rate at recruitment as the mean of the first three discharges (32). Finally, we estimated the discharge rate of each motor unit during the plateau. However, as shown in Fig. 3, time-dependent changes in discharge rate were observed during the plateau, with most of the GM motor units exhibiting a decrease in their discharge rate. Consequently, we used a sixth-order polynomial to smooth the instantaneous discharge rates (33) and then we considered the peak discharge rate from this polynomial fit.

We further assessed the difference in neural drive received by the three muscles by comparing their time-dependent changes in neural drive during the torque plateau. To this end, we estimated the neural drive through the calculation of the cumulative spike train (CST) of the identified motor units (26, 34). To generate the CST of each muscle, the individual motor unit discharge timings were summed and then smoothed with a Hanning window of 400-ms duration (35). After down-sampling the data by 100, we calculated the slope of the linear regression between CST and time to determine whether the CST decreased (negative slope different to 0), increased (positive slope different to 0), or remained stable during the torque plateau.

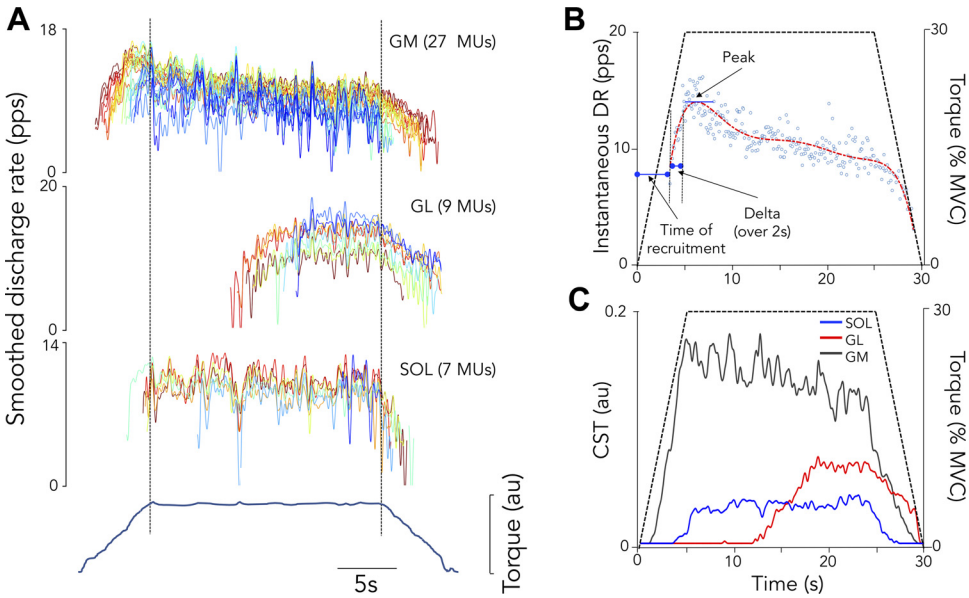

Figure 3. Individual example of the assessment of the neural drive during the isometric plantarflexions performed on the ergometer. *A*: represents the smoothed discharge rate (cut-off frequency = 2 Hz) of the motor units identified in *participant 11* during the contraction at 30% of MVC. *B*: shows three outcomes (time at recruitment, δ, and peak discharge rate) estimated from the instantaneous discharge rate of one motor unit of the gastrocnemius medialis muscle. Note that the peak discharge rate value was estimated from a sixth-order polynomial used to smooth the instantaneous discharge rates. *C*: shows the cumulative spike train (CST; index of neural drive) of each of the three muscles. GL, gastrocnemius lateralis; GM, gastrocnemius medialis; MVC, maximal voluntary contraction; SOL, soleus (medial-posterior compartment).

To determine whether the feet configuration (toes neutral and toes in) adopted during the heel-raise tasks could differentially affect GM and GL recruitment, we calculated the mean motor unit discharge rate. Values of discharge rate < 4 pps were removed from this calculation, as such discharge rates likely indicate inconsistent firings of the motor units (31). Note that SOL motor units were not considered in this part of the experiment, as it is already well known that the SOL and gastrocnemii muscles can be differentially activated by modifying the knee angle (36, 37), as is expected given their different function around the knee.

Statistical Analysis

A Shapiro–Wilk test was used to test for a normal distribution. The discharge rate data measured during the heel-raise task (toes in and toes neutral conditions) did not pass the normality test. Therefore, these data were transformed [1/square root(x)]. The distributions of the time at recruitment and δ discharge rate values did not pass the normality test either. However, because no transformation was able to provide a normal distribution, we performed nonparametric tests on these data. All data are reported as means ± SD, and the level of significance was set at $P \leq 0.05$.

Statistical analyses were performed in Statistica v. 7.0 (StatSoft, Tulsa, OK). The within-muscle coherence analysis was only performed when four or more motor units were identified. Consequently, the number of participants considered for this analysis differed between muscles. For this reason, we used a one-way ANOVA for independent samples to compare the PCI between muscles [between-subject factor: muscle (GM, GL, SOL)].

It is likely that different populations of motor units, with different intrinsic properties, were identified during the plantarflexion tasks performed at the different intensities (10%, 20%, and 50%). For this reason, we did not directly compare the time at recruitment and the δ discharge rate between intensities, and these values were only compared between muscles using a Kruskal–Wallis test for main effect [between-subject factor: muscle (GM, GL, SOL)]. When appropriate, post hoc analyses were performed using multiple comparisons of mean ranks.

The peak motor unit discharge rate estimated from the polynomial fit during the isometric plantarflexions was compared between muscles and contraction intensities using a two-way ANOVA [between-subject factor: muscle (GM, GL, SOL) and intensity (10%, 20%, and 50%)]. A similar two-way ANOVA was performed to test the effect of the feet position on the discharge rate of GL and GM [between-subject factor: muscle (GM, GL, SOL) and condition (toes neutral and toes in)]. When appropriate, post hoc analyses were performed using the Bonferroni test.

RESULTS

The entire data set (raw and processed data) is available at https://doi.org/10.6084/m9.figshare.12126627.

Motor Unit Decomposition

First, the spike-triggered averaging technique was used to identify decomposed motor units, which might originate from cross talk of one of the two other muscles. To achieve this aim, we compared the amplitude of the ensemble-averaged motor unit action potentials. At this stage, 17 motor units that were identified from the array placed above the GL (≈4% of the total number of GL motor units) were suspected to originate from GM. After exclusion of these motor units, the number of decomposed units over each of the five motor tasks ranged from 173 to 335 for GM, 10 to 120 for GL, and 65 to 94 for SOL (Table 1). Note that only 10 motor units were decomposed for GL from the isometric plantarflexion performed at 10% of MVC, which is consistent with the low global GL EMG amplitude measured at this contraction intensity, i.e., 7.1 ± 2.4% of the maximal EMG amplitude measured during MVC. The pulse-to-noise ratio averaged over the three muscles and the five tasks (i.e., a total of 2096 motor units) was 36.2 ± 4.5 (range, 30.0–53.6).

We used a coherence analysis to provide insight into the common neural drive received by the motor neurons. Because the number of GL motor unit discharges identified during the isometric plantarflexion tasks was too low (see METHODS), the coherence analysis was only performed on the isometric heel-raise task performed with toes in neutral position (toes neutral). Of note, the normalized global EMG amplitude of GM and GL (GM, 24.1 ± 6.0%; GL, 12.1 ± 6.9%; and SOL, 24.8 ± 10.7% of maximal EMG amplitude) during the toes neutral condition was close to that measured during the isometric plantarflexion at 30% of MVC (GM, 28.7 ± 6.8%; GL, 14.9 ± 4.7%; and SOL, 18.4 ± 11.5% of maximal EMG amplitude).

Within-Muscle Coherence

After discarding the motor units that were recruited intermittently and the data from participants with less than four consistently firing motor units, the within-muscle coherence analysis was performed on 243 motor units from 17 participants for GM, 83 motor units from 11 participants for GL, and 63 motor units from 10 participants for SOL.

The proportion of common synaptic input (PCI) with respect to the total input received by the motor neuron pool was estimated from the relationship between the average values of coherence in the bandwidth 0–5 Hz and the number of motor units used in the calculation (see METHODS; Fig. 2). As the number of participants differed between the three muscles, we ran a one-way ANOVA for independent samples. There was a significant main effect of *muscle* [$F(2, 35) = 14.2$, $P < 0.001$] on the PCI values, with the PCI being lower in SOL (0.58 ± 0.06) than in both GM (0.67 ± 0.06; $P = 0.004$) and GL (0.73 ± 0.07, $P < 0.001$) (Fig. 4). PCI was not different between GM and GL ($P = 0.063$). Note that we also ran a repeated-measures ANOVA on the seven participants who had enough active motor units discriminated from all the three muscles. This test confirmed the existence of a significant main effect of *muscle* [$F(2, 12) = 26.9$, $P < 0.001$], with the PCI being lower in SOL than in both GM ($P = 0.001$) and GL ($P < 0.001$), with no difference between GM and GL ($P = 0.082$).

The proportion of common input to motor neurons within the VL and VM, assessed on two participants who performed an isometric body-weight squat (additional experiments), was in the lower range of that calculated for the *triceps surae* muscles, i.e., VL, 0.50 and 0.57; VM, 0.49 and 0.54.

Table 1. *Number of decomposed motor units*

	GM		GL		SOL	
	Number	Means ± SD (range)	Number	Means ± SD (range)	Number	Means ± SD (range)
Plantarflexion10% MVC	294	17.3 ± 8.2 (*1–30*)	10	0.6 ± 0.9 (*0–3*)	92	5.8 ± 4.2 (*0–14*)
Plantarflexion30% MVC	275	16.2 ± 8.6 (*3–31*)	90	5.3 ± 4.5 (*0–13*)	94	5.9 ± 4.1 (*0–12*)
Plantarflexion50% MVC	173	10.2 ± 7.6 (*0–22*)	75	4.4 ± 5.6 (*0–21*)	65	4.1 ± 3.4 (*0–11*)
Heel raiseToes neutral	335	19.7 ± 9.5 (*6–36*)	120	7.1 ± 5.7 (*0–19*)	76	5.1 ± 4.1 (*0–15*)
Heel raiseToes in	312	18.4 ± 7.6 (*6–31*)	85	5.0 ± 3.9 (*0–12*)	—	—

Because of technical reasons, there were no data for *participant 14* during the isometric plantarflexions and for *participant 2* during the heel raise with the toes in neutral condition. In addition, soleus recordings are missing for one and two participants during the plantarflexions and the heel-raise conditions, respectively. Consequently, GM and GL data are reported for $n = 17$ participants (isometric plantarflexions and isometric heel raise with the toes in neutral condition); SOL data are reported for $n = 16$ (isometric plantarflexions) and $n = 15$ (isometric heel raises) participants. GL, gastrocnemius lateralis; GM, gastrocnemius medialis; MVC, maximal voluntary contractions; SOL, soleus.

Between-Muscles Coherence

When considering data from all participants, there was no significant correlation between the coherence in the bandwidth 0–5 Hz [common drive (28)] and the minimal number of motor units over the two muscles being tested ($r = 0.03$, −0.15, and −0.08 for the GM-GL, GL-SOL, and GM-SOL pair, respectively). This provides evidence that the number of motor units considered in the analysis did not influence the level of coherence that is reported. Consequently, after discarding the motor units that were recruited intermittently, we retained all the participants with at least one motor unit per muscle. Using this criterion, the coherence analysis was performed on 13 participants for GM-GL [193 (GM) and 87 (GL) motor units] and 11 participants for both GM-SOL [168 (GM) and 56 (SOL) motor units] and GL-SOL [62 (GL) and 52 (SOL) motor units].

Overall, minimal between-muscle coherence was observed, regardless of the bandwidth, i.e., δ (0–5 Hz), α (5–15 Hz), and β (15–35 Hz) bands. For example, when considering the GM-GL muscle pair, only two of 13 participants exhibited significant coherence over the entire bandwidth 0–5 Hz (Figs. 5 and 6). Whereas five of 13 participants exhibited coherence at some (but not all) frequencies within the 0–5 Hz bandwidth, six of 13 participants exhibited no significant coherence over this bandwidth. Note that *participant 5*, who exhibited the highest coherence over the whole population (Fig. 5), was retested 2 mo after the initial testing, and the results confirmed the presence of significant coherence. When considering the GM-SOL and GL-SOL muscle pairs, none of the participants exhibited significant coherence over the entire bandwidth 0–5 Hz (Figs. 5 and 6).

Note that the two participants who performed an isometric body-weight squat (additional experiments) exhibited significant coherence between VL and VM motor units, over the entire bandwidth 0–5 Hz (peak values, 0.34 and 0.81). It confirms previous results showing a strong common drive between these muscles during isometric knee extension tasks (11).

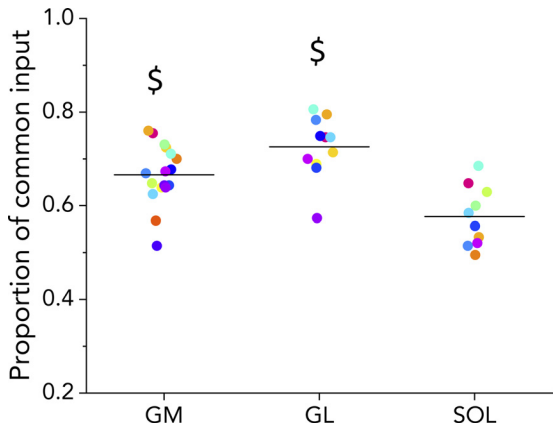

Figure 4. Proportion of common synaptic input to motor neurons within the same muscle, estimated during the isometric heel raise (toes neutral). The within-muscle coherence analysis was performed on 17, 11, and 10 participants for gastrocnemius medialis (GM), gastrocnemius lateralis (GL), and soleus (SOL), respectively. Each participant is represented by a different color and the horizontal line indicates the mean value. $, indicates significant difference compared with SOL. There was no significant difference between GM and GL.

Motor Unit Discharge Characteristics during the Isometric Plantarflexion Tasks

As indicated earlier, only 10 motor units were decomposed from the GL muscle during the plantarflexion at 10% of MVC. As the comparison between GL and GM was the main purpose of this study, no further analysis was completed on the contractions at 10% of MVC.

At 30% of MVC, most of the identified motor units discharged during the three contractions (93% for GM, 69% for GL, and 68% for SOL). There was a significant main effect of *muscle* on the time at recruitment ($H = 68.7$, df = 2, $P < 0.001$), with the GL motor units being recruited much later (11.5 ± 5.9 s) than both GM (4.4 ± 3.3s, $P < 0.001$) and SOL motor units (5.2 ± 4.2 s, $P < 0.001$). No difference of time at recruitment was observed between GM and SOL ($P = 0.20$). As the time at recruitment was calculated from the start of the 5-s ramp-up period (see METHODS), this result indicates that most of the motor units from GL started to be recruited during the torque plateau (Fig. 7). There was a significant main effect of *muscle* on the δ discharge rate measured during the first 2 s after recruitment ($H = 17.2$, df = 2, $P = 0.002$). The δ discharge rate was significantly lower for SOL (1.4 ± 0.9 pps · S^{-1}) than for both GL (1.8 ± 1.5 pps · S^{-1}, $P = 0.012$) and GM (2.0 ± 1.3 pps · S^{-1}, $P < 0.001$). No difference between GL and GM was observed ($P = 1$).

Similar results were observed for the contractions performed at 50% of MVC, with a significant main effect of *muscle* on the time at recruitment ($H = 80.7$, df = 2, $P < 0.001$). As observed at 30% of MVC, GL motor units were recruited

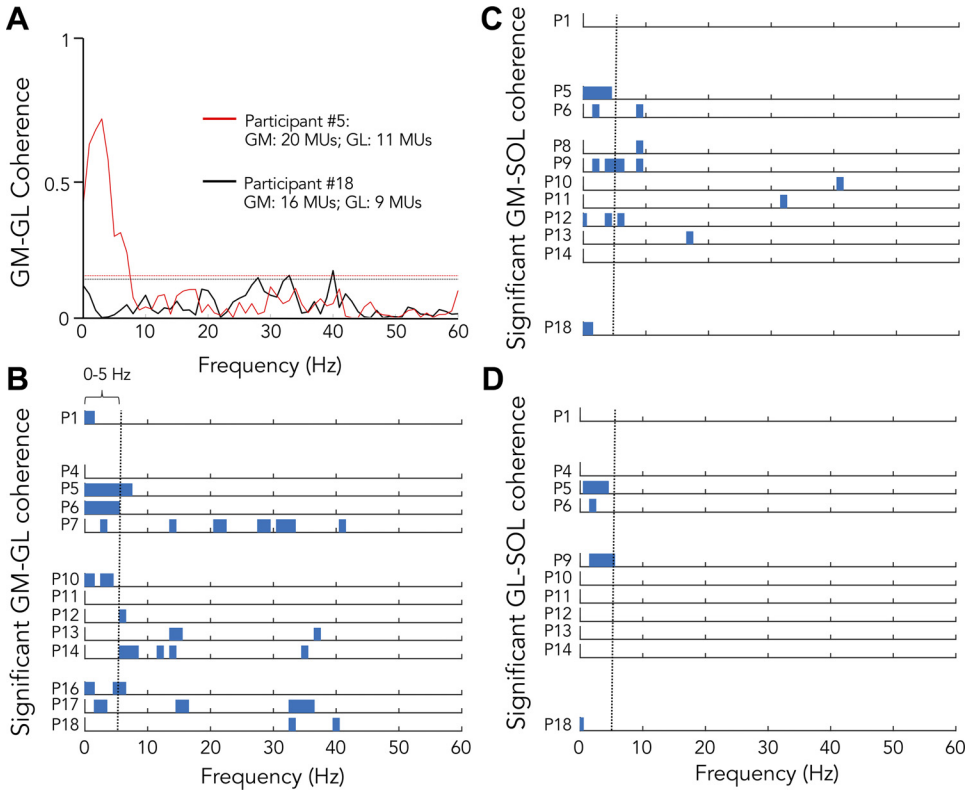

Figure 5. Between-muscle coherence estimated during the isometric heel raise (toes neutral). *A*: shows examples of the coherence between GM and GL for two participants: *participant 18* who exhibited no coherence and *participant 5* who exhibited the highest coherence over the population tested. The horizontal lines represent the threshold of significance defined as the highest coherence value for frequencies > 100 Hz, at which no coherence is expected. The other panels show, for each participant, the frequencies at which a significant coherence was observed for GM-GL (*B*), for GM-SOL (*C*), and for GL-SOL (*D*). Some participants were discarded from this analysis as too few motor units were discriminated to allow this analysis. Individual coherence data are depicted in Figs. 6. GL, gastrocnemius lateralis; GM, gastrocnemius medialis; SOL, soleus.

much later (9.5 ± 4.2 s) than both GM (3.7 ± 2.6 s, $P < 0.001$) and SOL motor units (4.4 ± 2.7 s, $P = 0.018$) (Fig. 7). At this intensity, SOL motor units were also recruited later than GM motor units ($P < 0.001$). There was also a main effect of *muscle* on the δ discharge rate ($H = 26.9$, df = 2, $P < 0.001$). The δ discharge rate was significantly lower for both SOL (1.5 ± 1.2 pps · S^{-1}, $P < 0.001$) and GL (1.6 ± 1.9 pps · S^{-1}, $P < 0.001$) when compared with GM (2.6 ± 1.6 pps · S^{-1}). There was no difference between GM and SOL ($P = 0.961$).

There was a significant main effect of *muscle* [$F(2, 766) = 83.4$, $P < 0.001$], a significant main effect of *intensity* [$F(1, 766) = 68.9$, $P < 0.001$], and a significant *muscle* × *intensity* interaction [$F(2, 766) = 8.7$, $P = 0.002$] on the peak motor unit discharge rate estimated from the polynomial fit (Fig. 7). Regardless of the contraction intensity, the discharge rate was lower for SOL than for both GM and GL (all P values <0.037). While there was no difference in discharge rate between GM and GL at 30% of MVC ($P = 1$), the discharge rate was significantly higher for GM (14.0 ± 3.0 pps) than GL (12.2 ± 2.6 pps; $P < 0.001$) at 50% of MVC. This result is mainly explained by the absence of an increase in discharge rate of the GL motor units between the two intensities ($P = 1$).

We estimated the change in neural drive of each muscle during the plateau of the force-matched contractions through the assessment of the change in their cumulative spike trains (CST). When considering all the participants and the three contractions at 30% of MVC, we observed a significant decrease in the GM CST for most of the contractions (48% decrease vs. 42% increase and 10% no change). Conversely, a significant increase in the CST was observed in 92% of the contractions for GL and 54% of the contractions for SOL. Opposite change in CST was observed in 64%, 65%, and 44% of the contractions when considering GM-GL, GM-SOL, and GL-SOL pair, which provides strong evidence for opposing changes in neural drive to these muscle pairs.

When considering the contractions at 50% of MVC, we observed a significant decrease in the GM and SOL CST for most of the contractions (69% and 71% for GM and SOL, respectively). Conversely, a significant increase in the GL CST was observed in 100% of the contractions. Opposite change in CST was observed in 66%, 36%, and 67% of the contractions when considering GM-GL, GM-SOL, and GL-SOL pairs.

Effect of Toe Position on Motor Unit Discharge Rate during Isometric Heel Raise

We compared the discharge rate of all identified motor units during the heel-raise tasks between toes neutral (335 and 120 motor units for GM and GL, respectively) and toes in (312 and 85 motor units for GM and GL, respectively) (Fig. 8). There was a significant main effect of *condition* [$F(1, 848) = 7.4$, $P = 0.006$], a significant main effect of *muscle* [$F(1, 848) = 12.7$, $P < 0.001$], and a significant *muscle* × *condition* on the discharge rate [$F(1, 848) = 10.5$, $P = 0.001$]. While no change in motor units discharge rate was observed for GM between the two conditions ($P = 1$), there was a significant increase in the discharge rate of GL motor units, from 10.2 ± 1.2 pps for toes neutral to 10.8 ± 1.5 pps for toes in ($P = 0.002$).

DISCUSSION

We identified strong common neural drive to the motor neuron pools innervating each muscle but minimal common

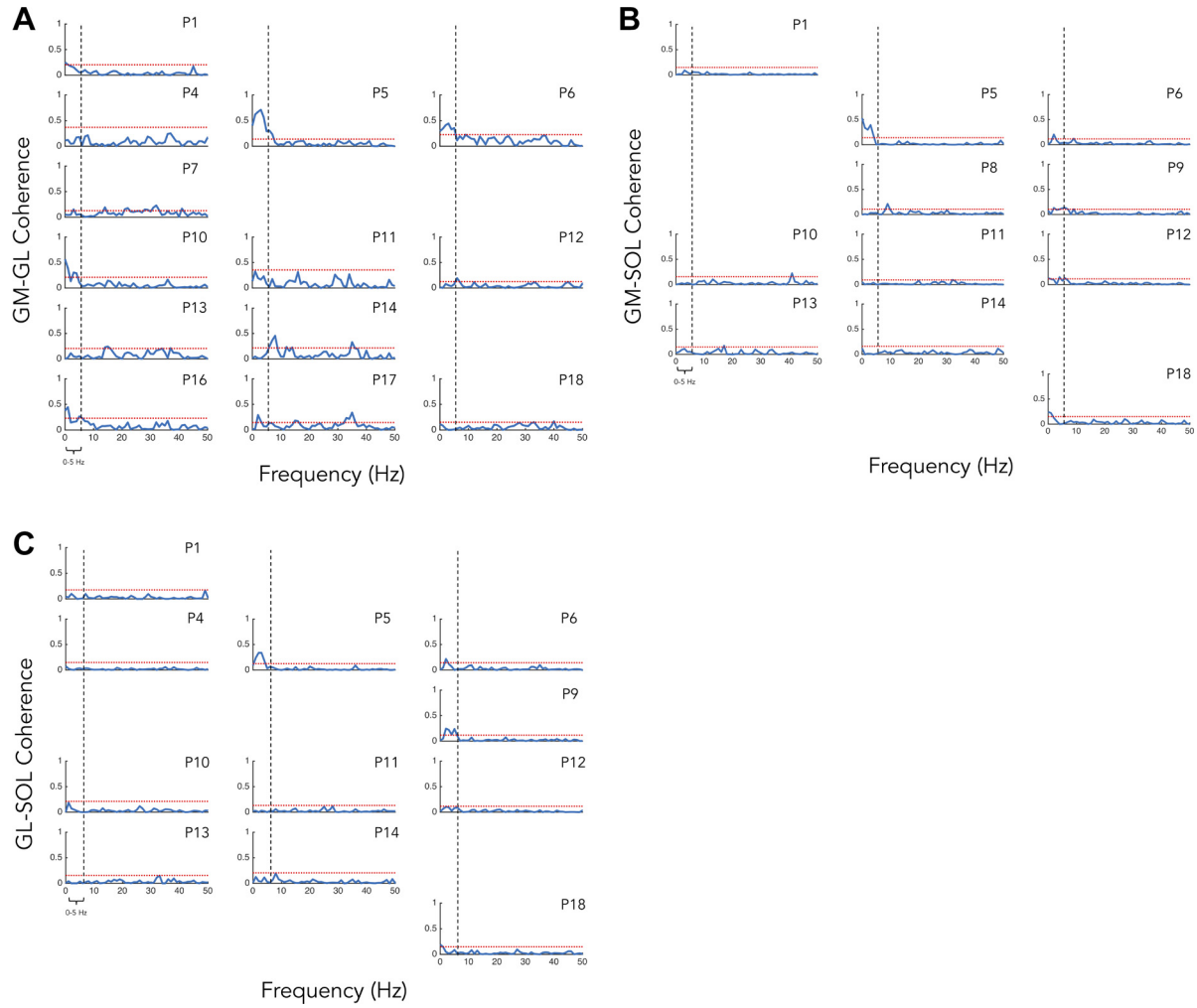

Figure 6. Individual data of coherence between the three heads of the triceps surae estimated during the isometric heel raise (toes neutral). The red horizontal lines represent the threshold of significance defined as the highest coherence value for frequencies > 100 Hz, at which no coherence is expected. Some participants were discarded from this analysis as too few motor units were discriminated to allow this analysis. GL, gastrocnemius lateralis; GM, gastrocnemius medialis; SOL, soleus. *A*: GM-GL coherence; *B*: GM-SOL coherence; *C*: GL-SOL coherence.

drive between pools innervating different muscles. Together with differences in motor unit behaviors, our results provide evidence for minimal common drive between the muscle heads of the triceps surae, which contrasts with observations from other anatomically derived synergist muscles. This important result has implications for our current understanding of the modular control of muscle coordination.

Strong Common Synaptic Input to Motor Neurons within Each Muscle

We assessed the PCI received by the motor neuron pools of the three muscles of the *triceps surae*. PCI values reported here were similar to those reported in the abductor digiti minimi, tibialis anterior, and vastus medialis (29). This suggests that motor neurons of a single muscle receive most of their input from a common source. Unlike the previous observations made by Negro, Yavuz, and Farina (29), but in line with other data obtained from the first dorsal interosseous and the biceps brachii (32), we observed a significant difference between muscles, with GL (PCI = 0.73) and SOL (PCI = 0.58) having the highest and lowest PCI values, respectively. These between-muscle differences may be interpreted as differences in the effective neural drive that is converted to force, presumably underlying differences in the control of these muscles.

Minimal Level of Common Drive between the Heads of the Triceps Surae

We determined that the three heads of the *triceps surae* receive minimal common drive during isometric heel-raise tasks (toes neutral). To reach this conclusion, we performed a coherence analysis between the CST of each muscle (11, 25, 35). To the best of our knowledge, this is the first report minimal (or an absence of) coherence in all the frequency bands reflecting cortical and spinal inputs (20) between muscles that share the same main function(s) and that belong to the same muscle group. As such, it was important to rule out the possibility that our approach failed to identify existing coherence. First, the coherence analysis requires that the CST is calculated from several motor units such that the synaptic input is represented over a broad frequency range (38). Our analysis was performed on a relatively large number of units

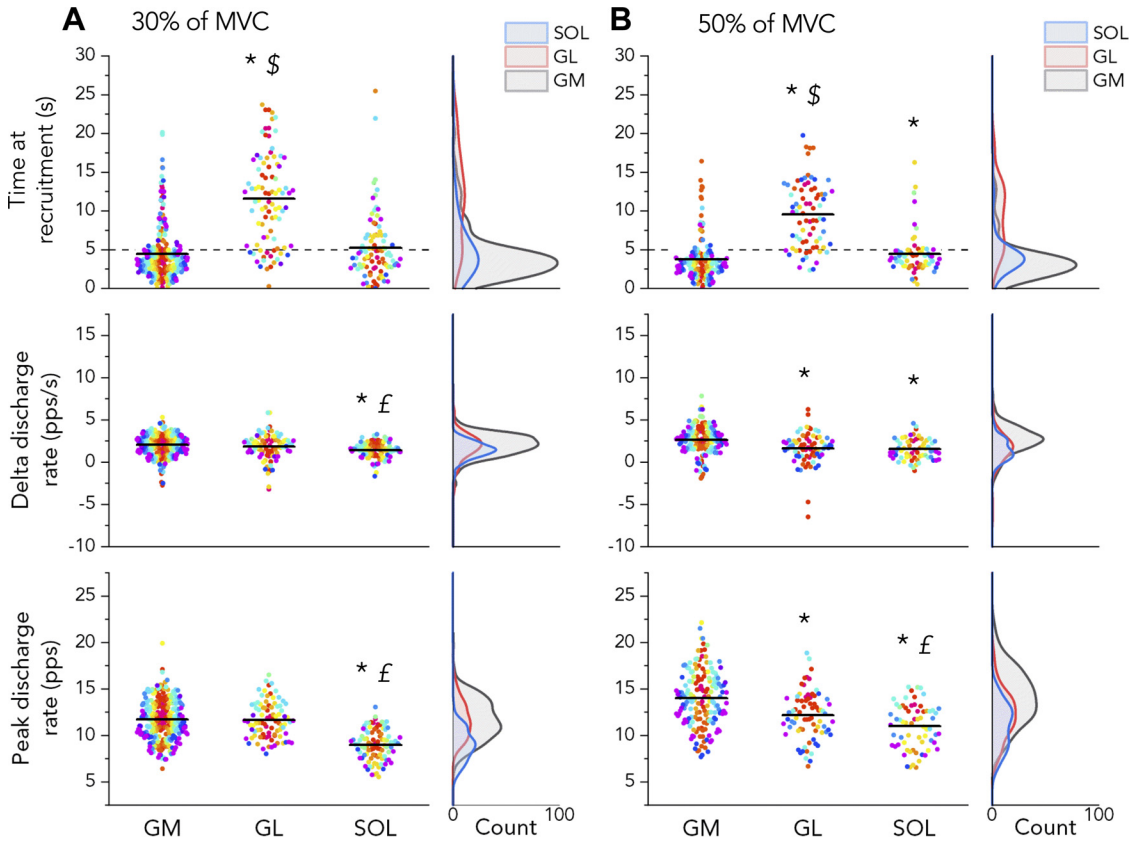

Figure 7. Motor unit discharge characteristics during the isometric plantarflexion tasks performed at 30% (*A*) and 50% of MVC (*B*). Each participant is represented by a different color, and the horizontal bar indicates the mean value. The dashed horizontal line on the upper panels indicates the beginning of the torque plateau. *$P < 0.05$ for comparison with GM; $$P < 0.05$ for comparison with SOL; £$P < 0.05$ for comparison with GL. GL, gastrocnemius lateralis; GM, gastrocnemius medialis; MVC, maximal voluntary contractions; SOL, soleus.

(Table 1) with, for example, 14.8 ± 7.3 (GM) and 6.7 ± 3.2 (GL) motor units when considering the coherence between GM and GL. It is important to note that some of the participants who exhibited no significant GM-GL coherence in the bandwidth 0–5 Hz (Fig. 5) were among the participants whose data allowed the largest number of motor units to be discriminated (e.g., 21 [GM] and 8 [GL] units for *participant 12*, 16 [GM] and 9 [GL] units for *participant 18*). Second, we tested our analysis procedure on the VL and VM muscles of two participants. In line with the strong common input shared

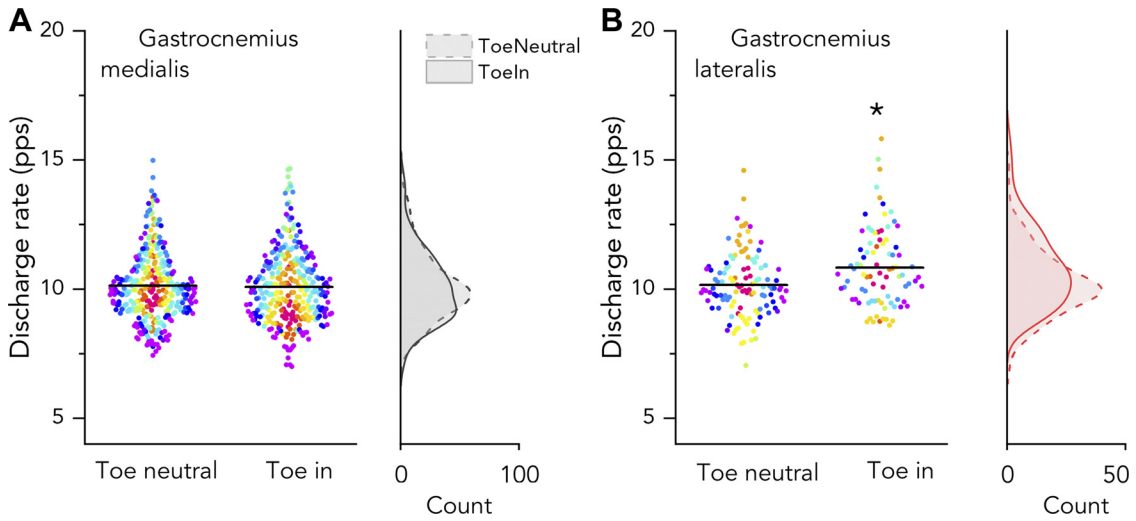

Figure 8. Discharge rate during the isometric heel raise performed with different feet configurations. Each participant ($n = 14–17$) is represented by a different color, and the horizontal bar indicates the mean value. *$P < 0.05$ for comparison with toes neutral. *A*: gastrocnemius medialis; *B*: gastrocnemius lateralis.

by these muscles (11), we observed a significant coherence in the bandwidth 0–5 Hz for both participants. Given the aforementioned considerations, we believe that our data set and analysis methods were appropriate to show coherence if it did exist between the muscles of the *triceps surae*.

Our conclusion that the three heads of the *triceps surae* share minimal common drive is further strengthened by two complementary approaches. First, the motor unit discharge characteristics observed during the isometric plantarflexion tasks performed on the ergometer revealed obvious differences among muscles. GL motor units were recruited much later than either SOL or GM motor units at both contraction intensities (Figs. 3 and 7). Even though this difference in recruitment time might be explained by different intrinsic motor neuron properties rather than different neural drive, the fact that opposite changes in CST were observed in most of the contractions provides evidence that the three muscles receive different neural drive (Fig. 3). Our proposition provides an explanation for the absence of active GL motor units observed during standing balance (18). Second, the differential change in the discharge rate of GL and GM observed between the heel-raise tasks performed with toes in and toes neutral provides definitive evidence that these muscles are not controlled primarily by shared neural drive, as it is the case for other synergist muscles.

GM and GL Are "Nonidentical Twins"

Even though SOL and gastrocnemii are consistently reported as part of the same synergy during walking (49), the observation that the SOL muscle does not share a common drive with the two gastrocnemius muscles is not surprising, given their different functions and previous observations of dissociated motor unit behavior of GM and SOL in humans (36, 37) and animals (39). However, considering that muscles that share the same function(s) are thought to share neural drive (9, 11), the minimal coherence between GM and GL, despite attaching to the same distal tendon, is somewhat surprising. Our findings do not support the long-held belief that GM and GL are the "same muscle" such that they are named the "twin" muscles in some languages, e.g., "jumeaux" in French and "gemelos" in Spanish.

The minimal common drive between GL and GM may be related to the complexity of ankle joint control. Control at the ankle is important in maintaining balance during a wide variety of tasks, such as quiet stance, walking, running, and maintaining balance when responding to perturbations. Therefore, relative independent control of these muscles may allow for flexible control of the ankle joint to comply with secondary goals (e.g., joint stabilization, distribution of tendon strain). This is supported by indirect neurophysiological and biomechanical measures of human GL and GM that suggest different actions in the frontal plane (16, 17, 40). Also, these muscles are architecturally different, with GL exhibiting a smaller volume and longer fascicles than GM (41). This means that these two muscles have different contractile dynamics (42). Therefore, an independent control of GM and GL might be an optimal way for the nervous system to tune the activation to the mechanical requirements of the task (43). Overall, the minimal common drive observed between GM and GL suggests that reducing the number of effectively controlled degrees of freedom may not always be the strategy used by the central nervous system to control movements, even when this strategy would be functionally viable. This is in agreement with recent results showing that the central nervous system compromises between restoration of task performance and optimization of joint load after VL denervation in rats (44). Of note, we cannot rule out an alternative interpretation that the lack of common drive between GM and GL is a suboptimal strategy resulting from the late, and perhaps incomplete, evolution of the Achilles tendon and plantarflexors for human locomotion (45).

Modular Organization of Muscle Coordination

It has been proposed that the central nervous system produces movements through the combination of motor modules; each module being composed of muscles activated by shared inputs to their motor neurons (3, 46, 47). However, the neural origin of motor modules is debated, with some studies suggesting that they reflect biomechanical constraints of the task rather than a neural control strategy (7, 48). Using a similar approach to that used in our study, shared neural drive was found between two thigh muscles for which control is biomechanically constrained [VL and VM; (11)] as well as between two hands muscles for which control is not biomechanically constrained [first dorsal interosseous and thenar muscles (25)]. Here, we observed little, if any, coherence in the bandwidth corresponding to both the spinal and cortical drive, suggesting that GM and GL are controlled mostly independently. Taken together, it provides evidence against a pure association between biomechanical constraints and modular muscle control. Indeed, GM and GL are both anatomically and biomechanically associated during plantarflexion, as performed in our study. However, these constraints did not determine modular control of their activation, even though control with reduced dimensionality would have been viable for these specific plantarflexion tasks. This and previous studies thus point to the possibility that neural connectivity may be partly dissociated from biomechanical connectivity.

It is important to note that classical noninvasive approaches, based on factorization of multiple bipolar EMG signals, consistently report GM and GL as part of the same module(s) (14, 15). Together with our results, this suggests that separate EMG signals can be correlated but in a way that does not reflect a common synaptic input (31). The noninvasive approach with EMG decomposition used in this study could be extended to other muscles to provide a comprehensive description of neural muscle modules that could be distinguished from "biomechanical" modules.

Limitations

This experiment requires consideration of several methodological aspects. First, the level of common synaptic input to the motor neuron pools of GM, GL, and SOL has been estimated only indirectly from the recorded motor neuron outputs. Moreover, in most cases, it was assumed that the transmission at the motor neuron population level was linear, as it has been proposed in previous work (38), although it cannot be excluded that transmission to the motor neuron output included some nonlinear components (49, 50). The coherence between the cumulative discharge times

calculated over a group of motor neurons reflects the common components of the synaptic input, although the frequency bands of these components may not be the same between input and output when accounting for nonlinear transmission. Similarly, the model we used to estimate the PCI does not specifically account for persistent inward currents, which introduce further nonlinearity in the system (49). Second, the SOL muscle is composed by four compartments with different architecture (51) and different innervation (52). Given the placement of our surface EMG electrodes (see METHODS), it is likely that we measured only one compartment, which did not represent the motor unit activity in the entire muscle. It is, therefore, possible that neural drive was shared between GM or GL and other SOL compartments. Finally, the observation of minimal common drive between the heads of the triceps surae cannot be extrapolated to other motor tasks such as dynamic tasks. Whether similar results would be observed during dynamic locomotor tasks remains an open question.

GRANTS

François Hug is supported by a fellowship from the Institut Universitaire de France (IUF) and a travel grant from the Société de Biomécanique. Support was received from the French national research agency (ANR-19-CE17-002-01, COMMODE project; to F. H.) and from the European Research Council Synergy Grant NaturalBionicS (Contract No. 810346 to D.F.).

DISCLOSURES

No conflicts of interest, financial or otherwise, are declared by the authors.

AUTHOR CONTRIBUTIONS

F.H., D.F., and K.J.T. conceived and designed research; F.H. and S.A. performed experiments; F.H., A.D. and S.A. analyzed data; F.H., A.D., D.F., and K.J.T. interpreted results of experiments; F.H. and S.A. prepared figures; F.H. and K.J.T. drafted manuscript; F.H., A.D., S.A., D.F., and K.J.T. edited and revised manuscript; F.H., A.D., S.A., D.F., and K.J.T. approved final version of manuscript.

ENDNOTE

At the request of the authors, readers are herein alerted to the fact that the entire data set (raw and processed data) is available at https://doi.org/10.6084/m9.figshare.12126627. These materials are not a part of this manuscript and have not undergone peer review by the American Physiological Society (APS). APS and the journal editors take no responsibility for these materials, for the website address, or for any links to or from it.

REFERENCES

1. **Bizzi E**, **Cheung VC**, **d'Avella A**, **Saltiel P**, **Tresch M.** Combining modules for movement. *Brain Res Rev* 57: 125–133, 2008. doi:10.1016/j.brainresrev.2007.08.004.
2. **Dominici N**, **Ivanenko YP**, **Cappellini G**, **d'Avella A**, **Mondi V**, **Cicchese M**, **Fabiano A**, **Silei T**, **Di Paolo A**, **Giannini C**, **Poppele RE**, **Lacquaniti F.** Locomotor primitives in newborn babies and their development. *Science* 334: 997–999, 2011. doi:10.1126/science.1210617.
3. **Tresch MC**, **Jarc A.** The case for and against muscle synergies. *Curr Opin Neurobiol* 19: 601–607, 2009. doi:10.1016/j.conb.2009.09.002.
4. **Overduin SA**, **d'Avella A**, **Carmena JM**, **Bizzi E.** Microstimulation activates a handful of muscle synergies. *Neuron* 76: 1071–1077, 2012. doi:10.1016/j.neuron.2012.10.018.
5. **Tresch MC**, **Bizzi E.** Responses to spinal microstimulation in the chronically spinalized rat and their relationship to spinal systems activated by low threshold cutaneous stimulation. *Exp Brain Res* 129: 401–416, 1999. doi:10.1007/s002210050908.
6. **Bizzi E**, **Cheung VC.** The neural origin of muscle synergies. *Front Comput Neurosci* 7: 51, 2013.
7. **Kutch JJ**, **Valero-Cuevas FJ.** Challenges and new approaches to proving the existence of muscle synergies of neural origin. *PLoS Comput Biol* 8: e1002434, 2012. doi:10.1371/journal.pcbi.1002434.
8. **Bremner FD**, **Baker JR**, **Stephens JA.** Correlation between the discharges of motor units recorded from the same and from different finger muscles in man. *J Physiol* 432: 355–380, 1991. doi:10.1113/jphysiol.1991.sp018389.
9. **Gibbs J**, **Harrison LM**, **Stephens JA.** Organization of inputs to motoneurone pools in man. *J Physiol* 485: 245–256, 1995. doi:10.1113/jphysiol.1995.sp020727.
10. **Kerkman JN**, **Daffertshofer A**, **Gollo LL**, **Breakspear M**, **Boonstra TW.** Network structure of the human musculoskeletal system shapes neural interactions on multiple time scales. *Sci Adv* 4: eaat0497, 2018. doi:10.1126/sciadv.aat0497.
11. **Laine CM**, **Martinez-Valdes E**, **Falla D**, **Mayer F Farina , D.** Motor neuron pools of synergistic thigh muscles share most of their synaptic input. *J Neurosci* 35: 12207–12216, 2015. doi:10.1523/JNEUROSCI.0240-15.2015.
12. **Lieb FJ**, **Perry J.** Quadriceps function. An anatomical and mechanical study using amputated limbs. *J Bone Joint Surg Am* 50: 1535–1548, 1968. doi:10.2106/00004623-196850080-00003.
13. **Winter SL**, **Challis JH.** Reconstruction of the human gastrocnemius force-length curve in vivo: part 1-model-based validation of method. *J Appl Biomech* 24: 197–206, 2008. doi:10.1123/jab.24.3.197.
14. **van den Hoorn W**, **Hodges PW**, **van Dieen JH**, **Hug F.** Effect of acute noxious stimulation to the leg or back on muscle synergies during walking. *J Neurophysiol* 113: 244–254, 2015. doi:10.1152/jn.00557.2014.
15. **Hug F**, **Turpin NA**, **Couturier A**, **Dorel S.** Consistency of muscle synergies during pedaling across different mechanical constraints. *J Neurophysiol* 106: 91–103, 2011. doi:10.1152/jn.01096.2010.
16. **Lee SS**, **Piazza SJ.** Inversion-eversion moment arms of gastrocnemius and tibialis anterior measured in vivo. *J Biomech* 41: 3366–3370, 2008. doi:10.1016/j.jbiomech.2008.09.029.
17. **Vieira TM**, **Windhorst U**, **Merletti R.** Is the stabilization of quiet upright stance in humans driven by synchronized modulations of the activity of medial and lateral gastrocnemius muscles? *J Appl Physiol (1985)* 108: 85–97, 2010. doi:10.1152/japplphysiol.00070.2009.
18. **Heroux ME**, **Dakin CJ**, **Luu BL**, **Inglis JT**, **Blouin JS.** Absence of lateral gastrocnemius activity and differential motor unit behavior in soleus and medial gastrocnemius during standing balance. *J Appl Physiol (1985)* 116: 140–148, 2014. doi:10.1152/japplphysiol.00906.2013.
19. **Farina D**, **Negro F.** Common synaptic input to motor neurons, motor unit synchronization, and force control. *Exerc Sport Sci Rev* 43: 23–33, 2015. doi:10.1249/JES.0000000000000032.
20. **Farmer SF**, **Bremner FD**, **Halliday DM**, **Rosenberg JR**, **Stephens JA.** The frequency content of common synaptic inputs to motoneurones studied during voluntary isometric contraction in man. *J Physiol* 470: 127–155, 1993. doi:10.1113/jphysiol.1993.sp019851.
21. **Holobar A**, **Zazula D.** Multichannel blind source separation using convolution kernel compensation. *IEEE Trans Signal Process* 55: 4487–4496, 2007. doi:10.1109/TSP.2007.896108.
22. **Holobar A**, **Farina D.** Blind source identification from the multichannel surface electromyogram. *Physiol Meas* 35: R143–165, 2014. doi:10.1088/0967-3334/35/7/R143.
23. **Holobar A**, **Minetto MA**, **Farina D.** Accurate identification of motor unit discharge patterns from high-density surface EMG and validation with a novel signal-based performance metric. *J Neural Eng* 11: e016008, 2014. doi:10.1088/1741-2560/11/1/016008.
24. **Del Vecchio A**, **Falla D**, **Felici F**, **Farina D.** The relative strength of common synaptic input to motor neurons is not a determinant of the maximal rate of force development in humans. *J Appl Physiol (1985)* 127: 205–214, 2019. doi:10.1152/japplphysiol.00139.2019.

25. **Del Vecchio A**, **Germer CM**, **Elias LA**, **Fu Q**, **Fine J**, **Santello M**, **Farina D.** The human central nervous system transmits common synaptic inputs to distinct motor neuron pools during non-synergistic digit actions. *J Physiol* 597: 5935–5948, 2019. doi:10.1113/JP278623.
26. **Del Vecchio A**, **Ubeda A**, **Sartori M**, **Azorin JM**, **Felici F**, **Farina D.** Central nervous system modulates the neuromechanical delay in a broad range for the control of muscle force. *J Appl Physiol (1985)* 125: 1404–1410, 2018. doi:10.1152/japplphysiol.00135.2018.
27. **Baker SN**, **Kilner JM**, **Pinches EM**, **Lemon RN.** The role of synchrony and oscillations in the motor output. *Exp Brain Res* 128: 109–117, 1999. doi:10.1007/s002210050825.
28. **De Luca CJ**, **LeFever RS**, **McCue MP**, **Xenakis AP.** Control scheme governing concurrently active human motor units during voluntary contractions. *J Physiol* 329: 129–142, 1982. doi:10.1113/jphysiol.1982.sp014294.
29. **Negro F**, **Yavuz US**, **Farina D.** The human motor neuron pools receive a dominant slow-varying common synaptic input. *J Physiol* 594: 5491–5505, 2016. doi:10.1113/JP271748.
30. **Baker SN**, **Pinches EM**, **Lemon RN.** Synchronization in monkey motor cortex during a precision grip task. II. effect of oscillatory activity on corticospinal output. *J Neurophysiol* 89: 1941–1953, 2003. doi:10.1152/jn.00832.2002.
31. **Martinez-Valdes E**, **Negro F**, **Falla D**, **De Nunzio AM**, **Farina D.** Surface electromyographic amplitude does not identify differences in neural drive to synergistic muscles. *J Appl Physiol (1985)* 124: 1071–1079, 2018. doi:10.1152/japplphysiol.01115.2017.
32. **Farina D**, **Castronovo AM**, **Vujaklija I**, **Sturma A**, **Salminger S**, **Hofer C**, **Aszmann O.** Common synaptic input to motor neurons and neural drive to targeted reinnervated muscles. *J Neurosci* 37: 11285–11292, 2017. doi:10.1523/JNEUROSCI.1179-17.2017.
33. **Gorassini M**, **Yang JF**, **Siu M**, **Bennett DJ.** Intrinsic activation of human motoneurons: possible contribution to motor unit excitation. *J Neurophysiol* 87: 1850–1858, 2002. doi:10.1152/jn.00024.2001.
34. **Negro F**, **Holobar A**, **Farina D.** Fluctuations in isometric muscle force can be described by one linear projection of low-frequency components of motor unit discharge rates. *J Physiol* 587: 5925–5938, 2009. doi:10.1113/jphysiol.2009.178509.
35. **De Luca CJ**, **LeFever RS**, **McCue MP**, **Xenakis AP.** Behaviour of human motor units in different muscles during linearly varying contractions. *J Physiol* 329: 113–128, 1982. doi:10.1113/jphysiol.1982.sp014293.
36. **Kennedy PM**, **Cresswell AG.** The effect of muscle length on motor-unit recruitment during isometric plantar flexion in humans. *Exp Brain Res* 137: 58–64, 2001. doi:10.1007/s002210000623.
37. **Lauber B**, **Lichtwark GA**, **Cresswell AG.** Reciprocal activation of gastrocnemius and soleus motor units is associated with fascicle length change during knee flexion. *Physiol Rep* 2: e12044, 2014. doi:10.14814/phy2.12044.
38. **Farina D**, **Negro F**, **Muceli S**, **Enoka RM.** Principles of motor unit physiology evolve with advances in technology. *Physiology (Bethesda)* 31: 83–94, 2016. doi:10.1152/physiol.00040.2015.
39. **Hodgson JA.** The relationship between soleus and gastrocnemius muscle activity in conscious cats–a model for motor unit recruitment? *J Physiol* 337: 553–562, 1983. doi:10.1113/jphysiol.1983.sp014641.
40. **Cohen JW**, **Gallina A**, **Ivanova TD**, **Vieira T**, **McAndrew DJ**, **Garland SJ.** Regional modulation of the ankle plantarflexor muscles associated with standing external perturbations across different directions. *Exp Brain Res* 238: 39–50, 2020. doi:10.1007/s00221-019-05696-8.
41. **Crouzier M**, **Lacourpaille L**, **Nordez A**, **Tucker K**, **Hug F.** Neuromechanical coupling within the human triceps surae and its consequence on individual force-sharing strategies. *J Exp Biol* 221: jeb187260, 2018. doi:10.1242/jeb.187260.
42. **Biewener AA.** Locomotion as an emergent property of muscle contractile dynamics. *J Exp Biol* 219: 285–294, 2016. doi:10.1242/jeb.123935.
43. **Hudson AL**, **Gandevia SC**, **Butler JE.** A principle of neuromechanical matching for motor unit recruitment in human movement. *Exerc Sport Sci Rev* 47: 157–168, 2019. doi:10.1249/JES.0000000000000191.
44. **Alessandro C**, **Rellinger BA**, **Barroso FO**, **Tresch MC.** Adaptation after vastus lateralis denervation in rats demonstrates neural regulation of joint stresses and strains. *Elife* 7, 2018. doi:10.7554/eLife.38215.
45. **Aerts P**, **D'Aout K**, **Thorpe S**, **Berillon G**, **Vereecke E.** The gibbon's Achilles tendon revisited: consequences for the evolution of the great apes? *Proc Biol Sci* 285, 2018.
46. **Berniker M**, **Jarc A**, **Bizzi E**, **Tresch MC.** Simplified and effective motor control based on muscle synergies to exploit musculoskeletal dynamics. *Proc Natl Acad Sci USA* 106: 7601–7606, 2009. doi:10.1073/pnas.0901512106.
47. **d'Avella A**, **Bizzi E.** Shared and specific muscle synergies in natural motor behaviors. *Proc Natl Acad Sci USA* 102: 3076–3081, 2005. doi:10.1073/pnas.0500199102.
48. **Valero-Cuevas FJ**, **Venkadesan M**, **Todorov E.** Structured variability of muscle activations supports the minimal intervention principle of motor control. *J Neurophysiol* 102: 59–68, 2009. doi:10.1152/jn.90324.2008.
49. **Binder MD**, **Powers RK**, **Heckman CJ.** Nonlinear input-output functions of motoneurons. *Physiology (Bethesda)* 35: 31–39, 2020. doi:10.1152/physiol.00026.2019.
50. **Watanabe RN**, **Kohn AF.** Fast oscillatory commands from the motor cortex can be decoded by the spinal cord for force control. *J Neurosci* 35: 13687–13697, 2015. doi:10.1523/JNEUROSCI.1950-15.2015.
51. **Bolsterlee B**, **Finni T**, **D'Souza A**, **Eguchi J**, **Clarke EC**, **Herbert RD.** Three-dimensional architecture of the whole human soleus muscle in vivo. *PeerJ* 6: e4610, 2018. doi:10.7717/peerj.4610.
52. **Loh EY**, **Agur AM**, **McKee NH.** Intramuscular innervation of the human soleus muscle: a 3D model. *Clin Anat* 16: 378–382, 2003. doi:10.1002/ca.10170.